Hard and Mid Energy X-ray Microprobes

Steve Sutton and Tony Lanzirotti

University of Chicago

GeoSoilEnviroCARS Sector at the Advanced Photon Source (IL)

Beamline X26A at the National Synchrotron Light Source (NY)

Some Science Drivers for X-ray Microprobes

Actinide Reactions and Transport:

- Speciation of these elements in contaminated materials in order to predict their mobilities and pathways in the subsurface.
- Diffusion and redox transformations in real systems (i.e., soils and sediments associated with contaminated sites)

Biogeochemistry of Metal Contaminants:

- Speciation of these metals in contaminated sediments
- Host phases of these metals in mine waste derived soils and other contaminated geomaterials in order to predict their human and ecological risks.
- Correlations between speciation, mineral hosts and human health factors.
- Chemistry of metals in amended soils and source materials to define the biogeochemical transport pathways.
- Phytoremediation-relevant studies of uptake by plants.

Crystal Chemistry:

- Crystal chemistry of energy-relevant elements
- Incorporation mechanisms of these elements in various compounds and minerals.
- Bonding environments of contaminants in potential encapsulation minerals.

Igneous and Hydrothermal Systems:

- Valence determinations by XANES as proxies for redox conditions of magmatic systems
- Speciation of metals in hydrothermal fluids (fluid inclusions)

Cosmochemistry

- Compositions of primitive solar system and interstellar materials

Common Applications of XRF Microprobes

- Spot XRF and XAFS analyses: microsamples (particles, fluid inclusions, etc) including composition and speciation; microregions in heterogeneous materials
- Compositional mapping (2D): chemical zoning, diffusion profiles, identification of reaction fronts, wetting properties of surfaces, elemental associations
- Fluorescence microtomography (2D/3D): same as above in tomographic mode
- MicroXRD: phase identification and correlation with elemental and speciation information from above

Arsenic Speciation and Mineralogy in Mine Wastes

H. Jamieson and S. Walker (Queen's University, Canada)

- 60 years of gold mining and processing has left the Yellowknife area of the Northwest Territories, Canada, with a complex environmental legacy of arsenic-bearing mine waste (tailings, roaster waste, waste rock, soils and lake sediments.
- Results: Much of the arsenic is hosted by roaster-generated iron oxides (hematite and maghemite) containing both As(III) and As(V), not arsenopyrite as previously thought.
- As(III) in the roaster iron oxide phases is persistent – present in 50 year old, unsaturated and oxidizing tailings, presenting a long term environmental hazard.

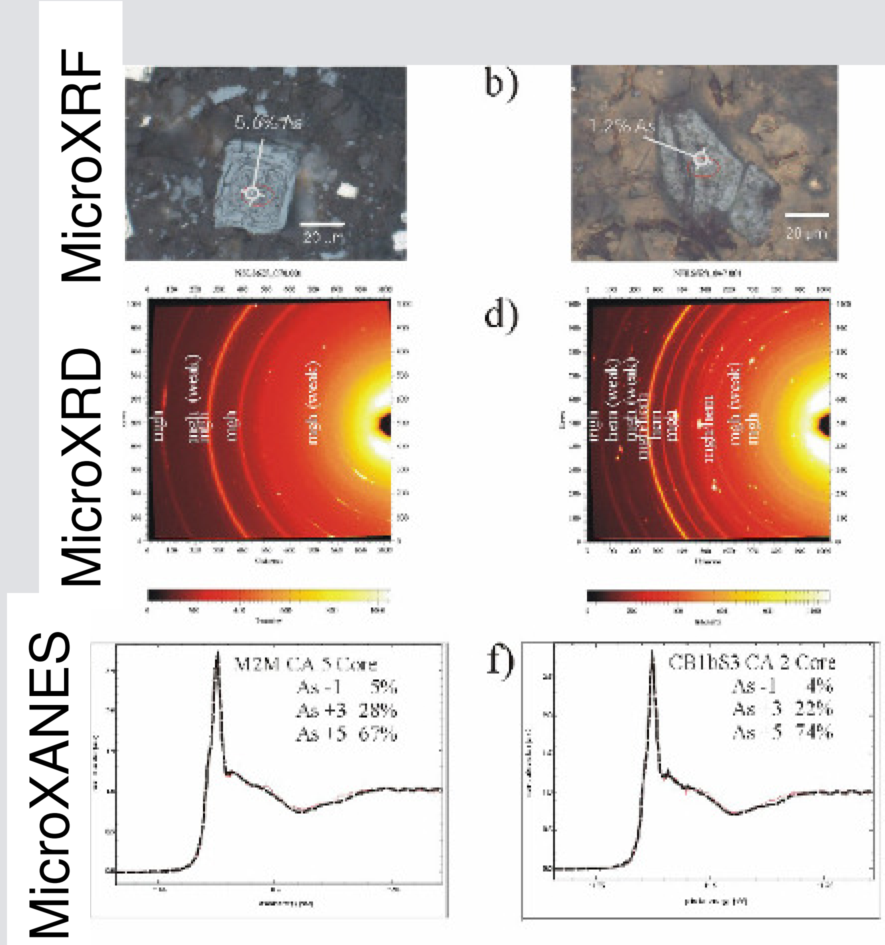

Walker, S.R., et al. (2005) Can. Min. 43, 1205-1224

Cesium Incorporation into Phyllosilicates

- Cs L_{α} map of muscovite cross section (1300 x 150 μm)
- "Non-edge" regions contain one-third of the Cs - associated with flake partings rather than interlayer lattice sites.
- Enhanced sorption capacity, transport limitation to desorption, increased overall immobilization

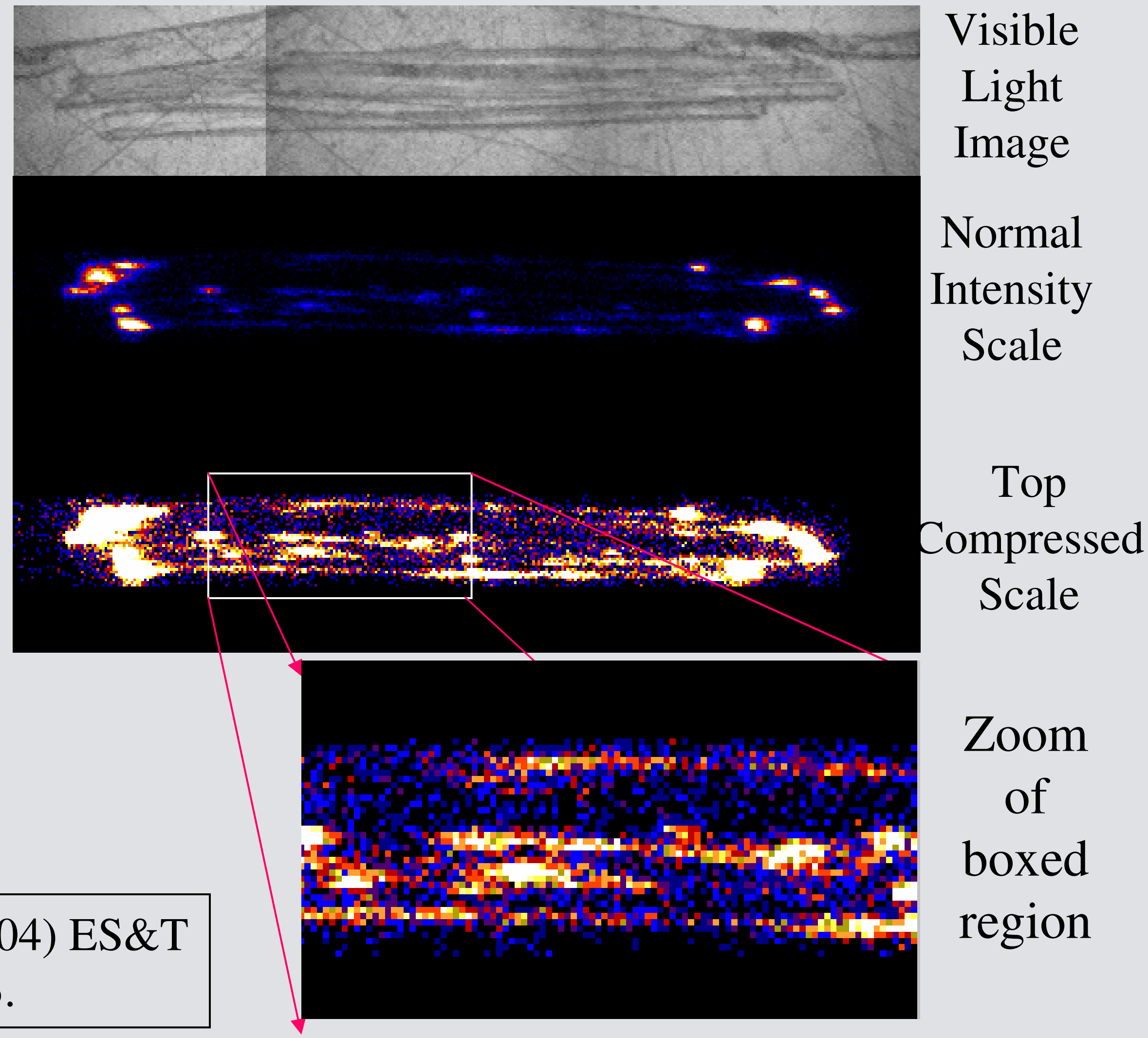

McKinley, J. P., et al. (2004) ES&T 38(4):1017-1023.

Diffusive Transport of Redox Sensitive Metals

T. Tokunaga (LBNL) et al.

- Understanding mobility and transport of fluid phases in the subsurface is important for predicting the behavior of contaminants in sediments, nuclear waste storage, the carbon cycle, and fossil energy resources.
- Multi-element interactions (e.g. Fe, Mn, Cr, U) are poorly understood.
- Current research targets several issues including: (1) effects of organic carbon (OC) forms and supply rates on stability of bioreduced U, (2) the roles of Fe(III)- and Mn(III,IV)-oxides as potential U oxidants in sediments.
- Redox transformations of U are being tested in sediment columns supplied with OC at variable rates in 200 mm long columns being infused with either lactate or acetate in synthetic groundwater.
- Columns ran for over 400 days.

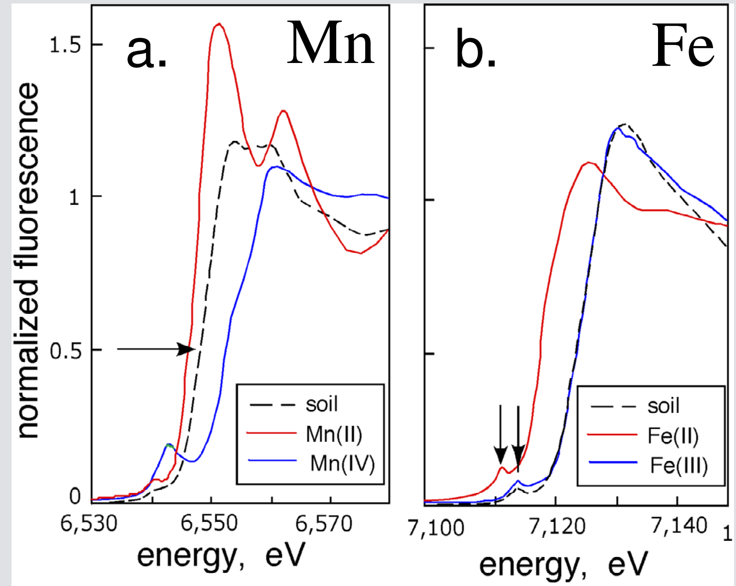

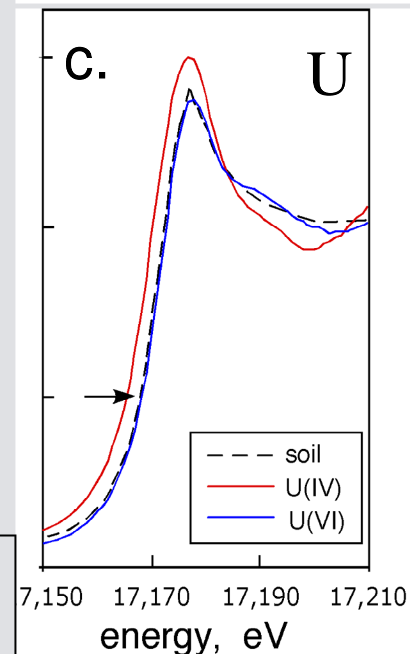

XANES spectra of original FRC2 sediment and end member oxidation state standards

- Mn(III,IV) oxides were completely reduced to Mn(II) in columns infused with OC
- Fe changed very little (~ 88% Fe(III)) under even the highest injected OC concentrations.
- In columns supplied with 160 and 550 mmol OC (kg sediment)$^{-1}$ year^{-1}, rapid U reduction was followed by a transient reoxidation period, before stabilizing in predominantly reduced state.
- Even at this late stage, about 20% of the U remained as U(VI).
- The measured rapid and complete Mn reduction, and very little reduction of a much larger Fe(III) inventory support the hypothesis (Wan et al., 2005) that a reactive Fe(III) fraction is responsible for U(IV) reoxidation under reducing conditions.

Wan, J., et al. (2005) Reoxidation of bioreduced uranium under reducing conditions. *Environ. Sci. Technol.*, *39*, 6162-6169.

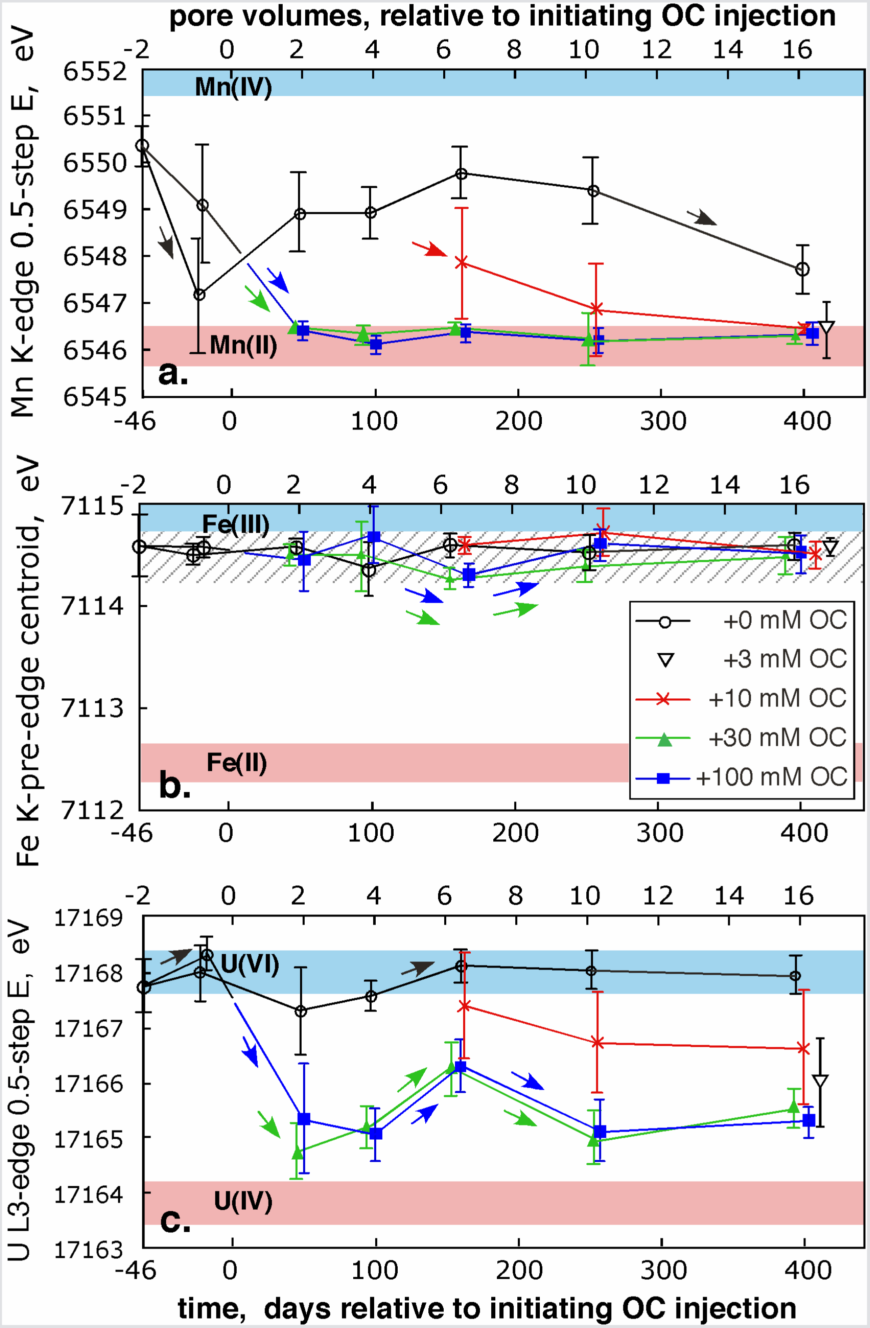

Localization of Iron in Arabidopsis Seed Requires the Vacuolar Membrane Transporter VIT1

Col-O

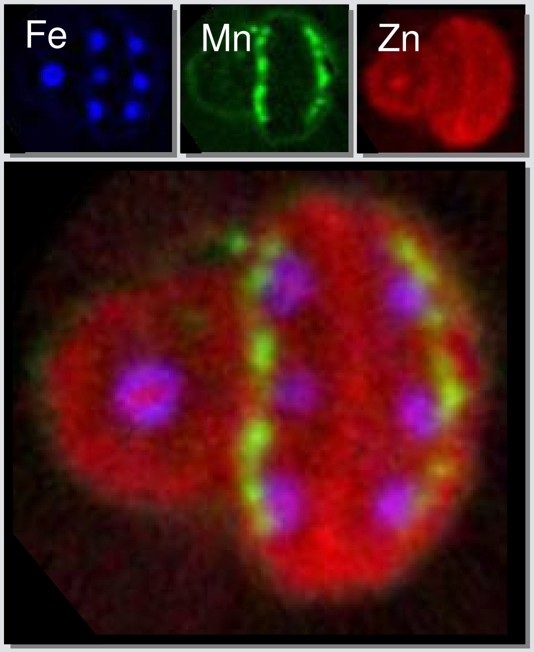

atvit1-1

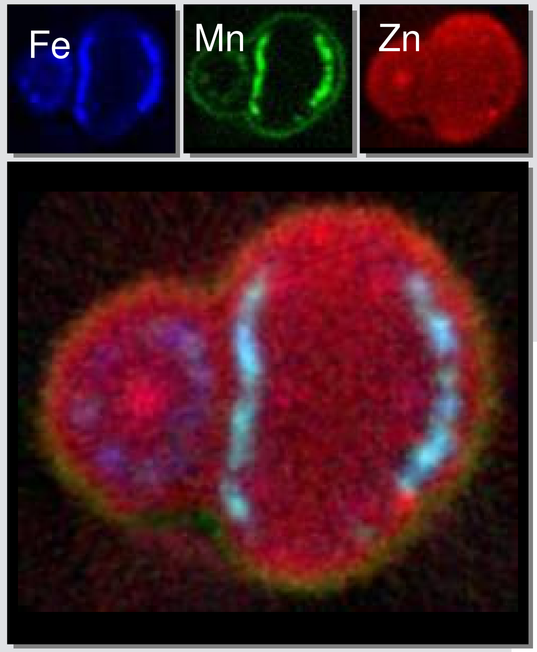

- **Ionomics:** the study of how genes regulate ions in cells.
- Fe deficiency most common nutritional disorder in the world

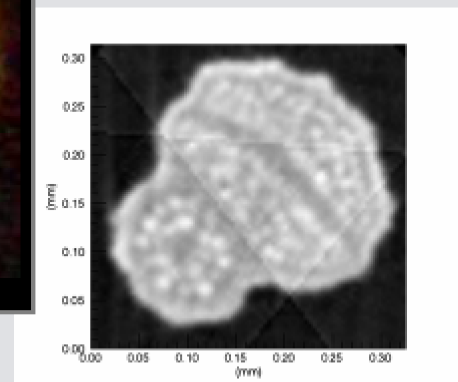

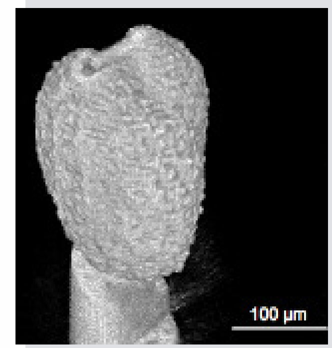

- Synchrotron x-ray fluorescence microtomography shows that the majority of iron is precisely localized to the provascular strands of the embryo. This localization of iron is completely abolished when the vacuolar iron uptake transporter VIT1 is disrupted, making vacuoles a promising target for increasing the iron content of seeds.

Kim, S., et al., (2006) Science, 314, 1295-1298.

Chemical Speciation in Hydrothermal Fluids

Linkam 1500 Heating Stage

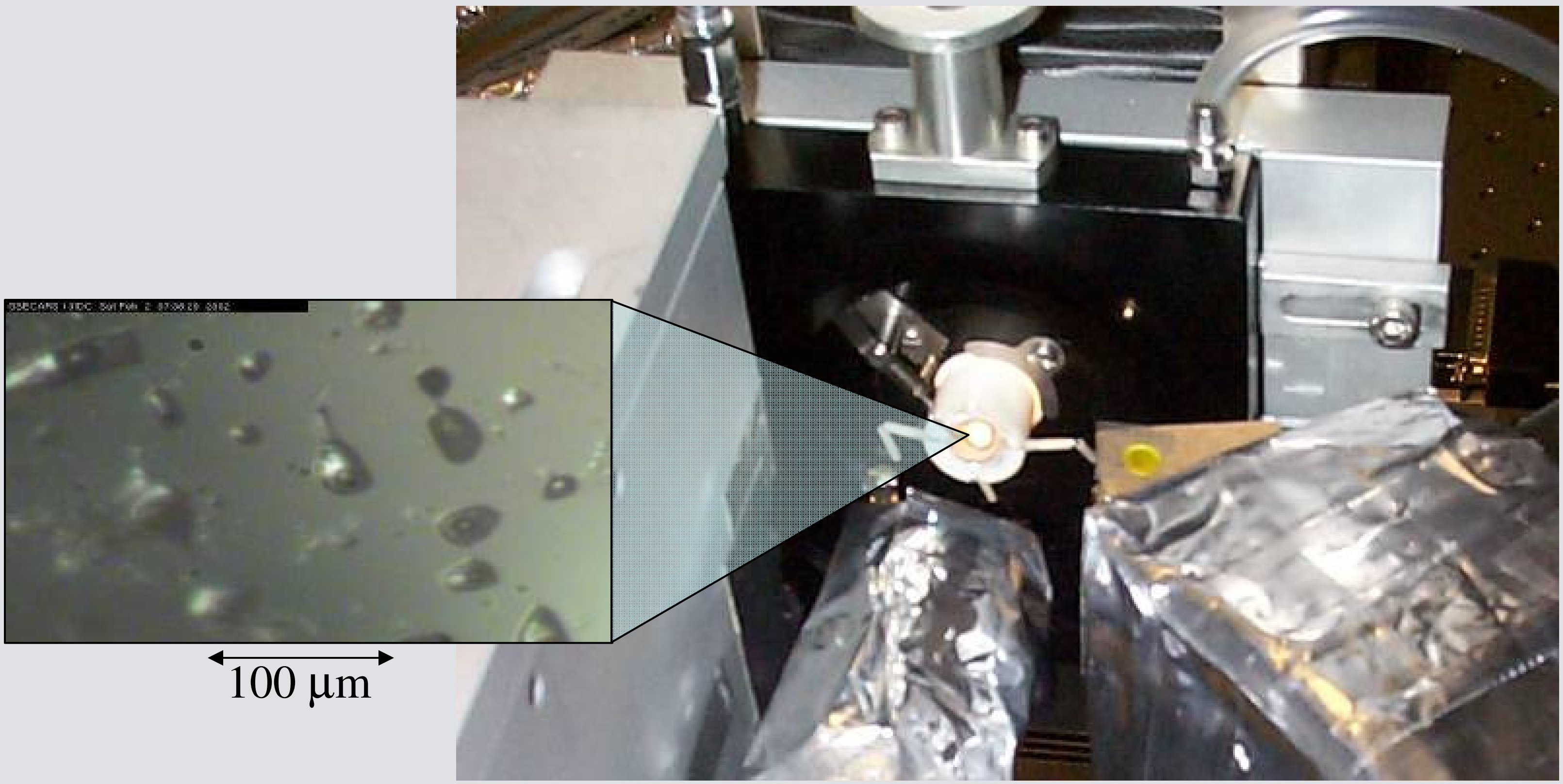

Fluid inclusion analyses at high temperature (to 1000 °C)

Cu XANES and EXAFS in Fluid Inclusions

Cu K-edge XANES in fluid inclusions:

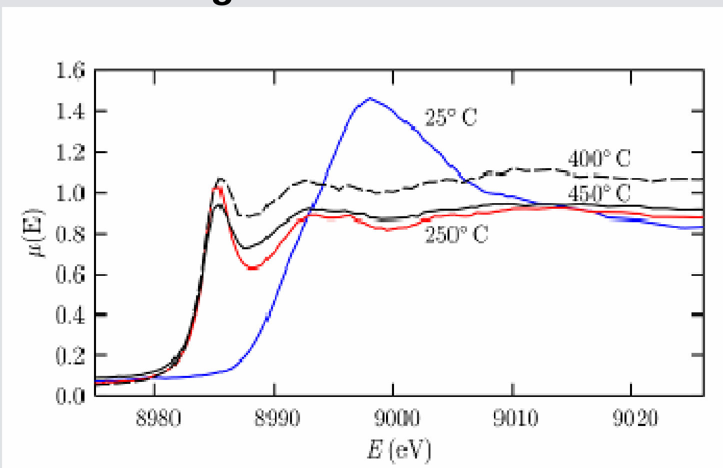

Cu EXAFS from high temp. phase

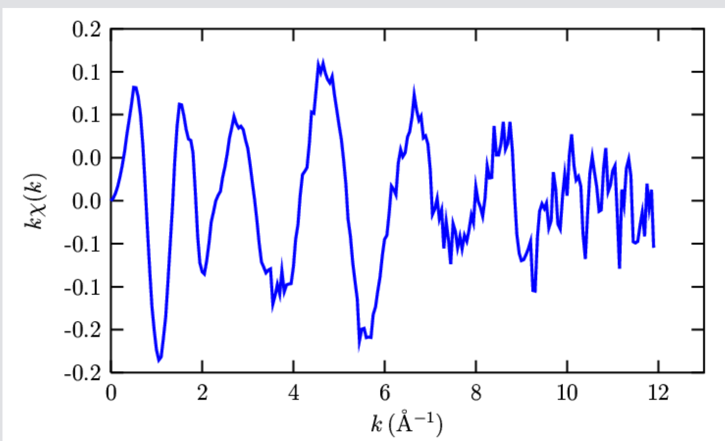

Mavrogenes, J., et al. (2002) Am. Min. 87, 1360

Vapor-phase inclusions show dramatic differences at low and high temperature:

Low temp: Cu^{2+} in aqueous solution

High temp: Cu^{1+} with Cl or S ligand.

These results are consistent with Fulton et al [Chem Phys Lett. 330, p300 (2000)] study of Cu in well controlled supercritical solutions

Quantitative EXAFS analysis of the high temperature phase confirmed that Cu is coordinated with either 2 Cl at ~2.08Å or 1 O at ~2.00Å and 1 Cl at ~2.09Å

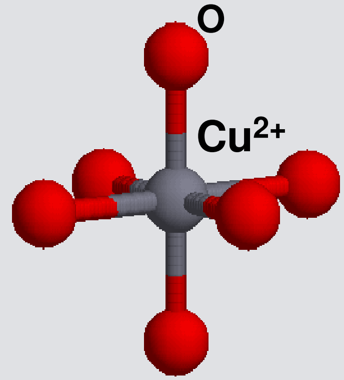

Low temp

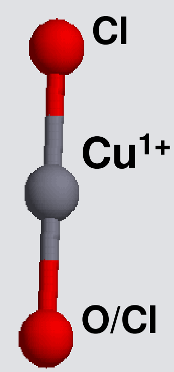

High temp

Pre-edge Peak Intensity-Oxygen Fugacity Calibration for Basaltic Glasses

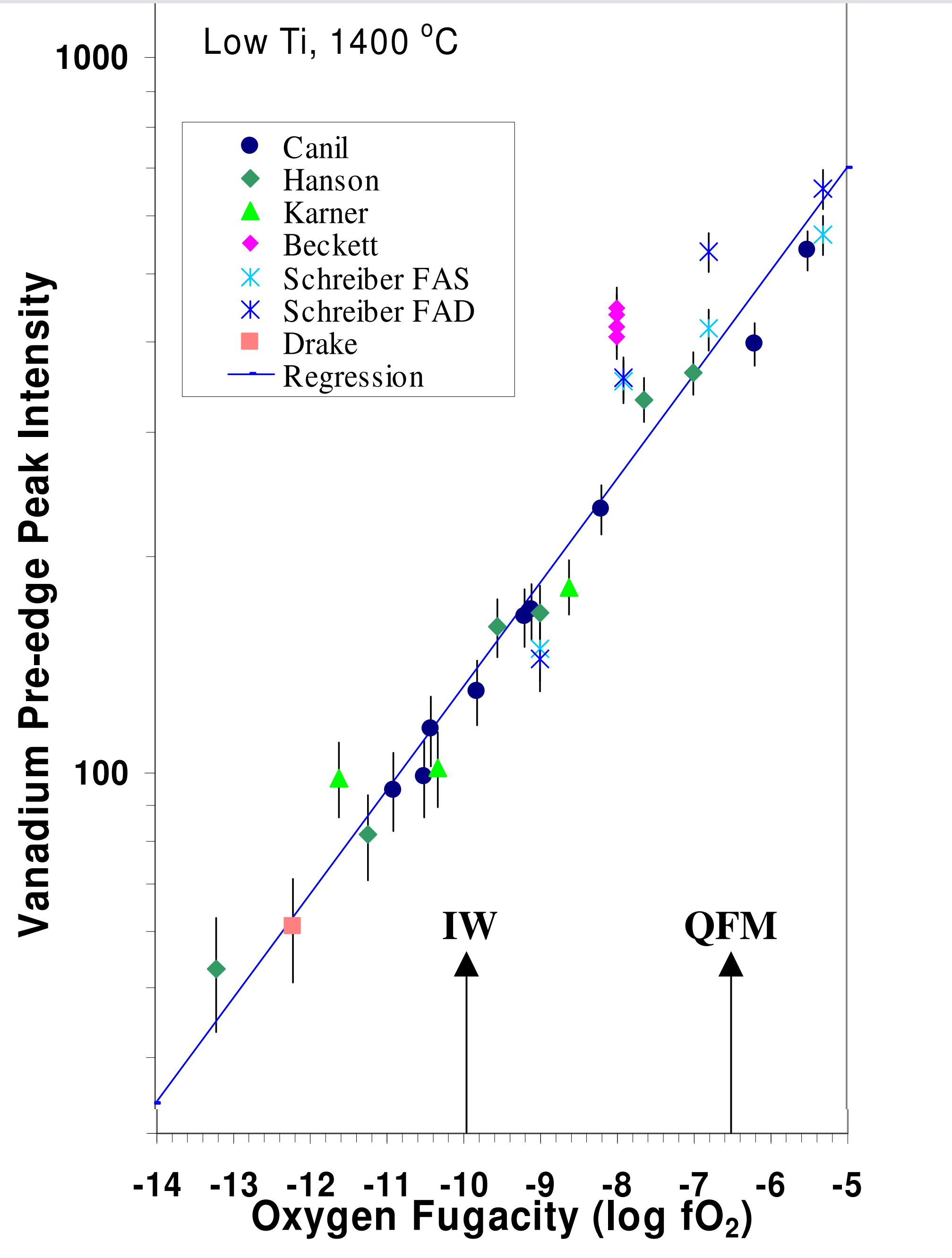

Sutton et al. (2005) GCA 69, 2333-2348.

Stardust Comet Dust

The Stardust Mission brought back samples from the comet Wild-2, embedded in aerogel.

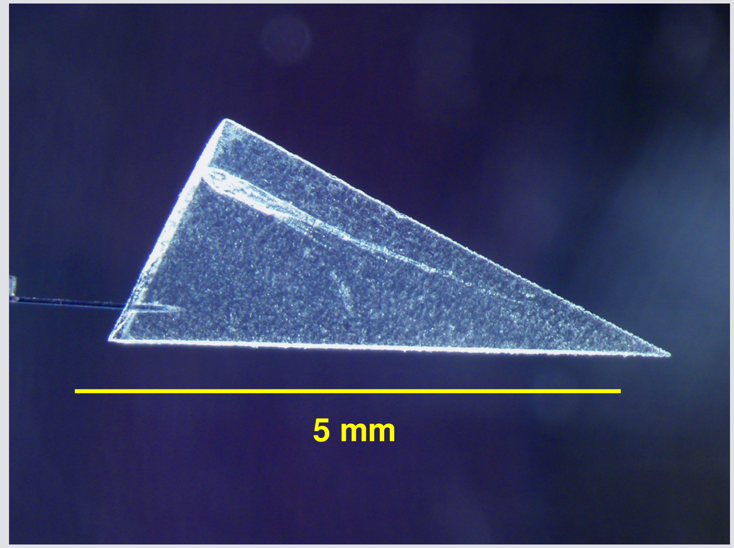

XRF mapping along the entire track shows that the elements are heterogeneous along the track, with Zn predominantly near the entry, and Cr near the terminal end.

Comet Wild-2 Track 3

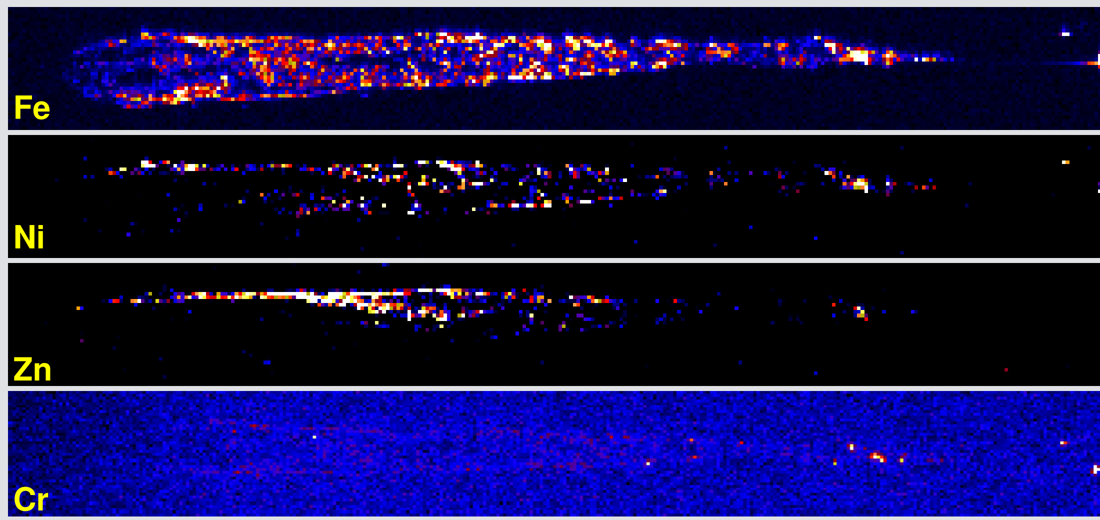

Flynn, G., and 80 others (2006) Elemental Compositions of Comet 81P/Wild 2 Samples Collected by Stardust. Science, 314, 1731-1735.

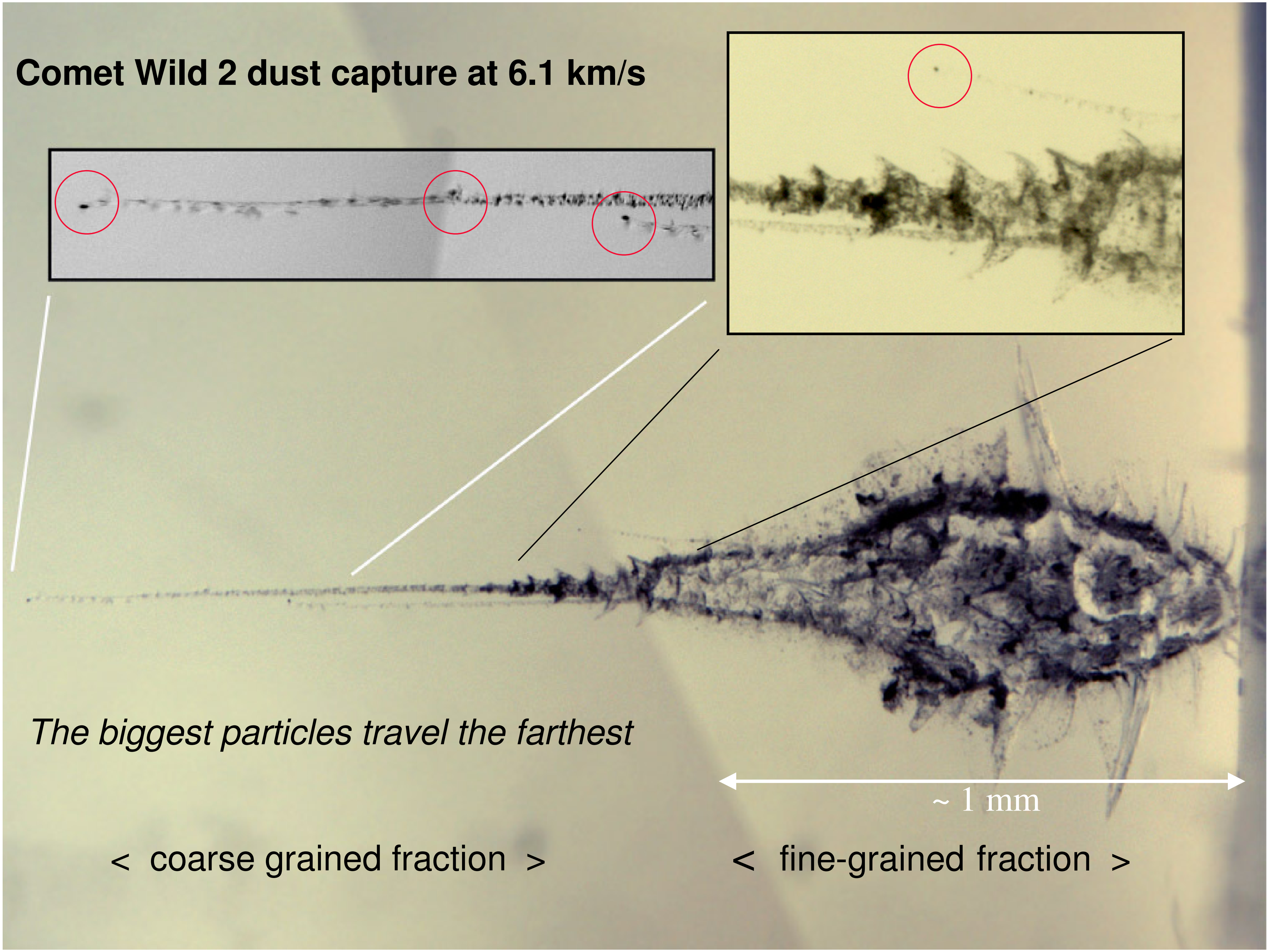
Comet Wild 2 dust capture at 6.1 km/s
The biggest particles travel the farthest
~ 1 mm
< coarse grained fraction >
< fine-grained fraction >

Composition of Fragments Along Track 3

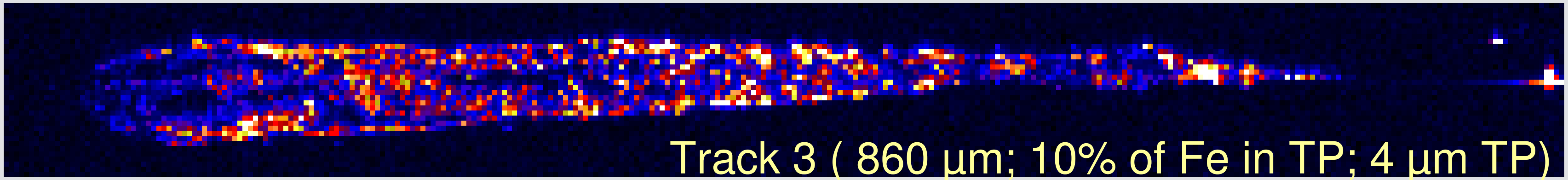

- The 20 most intense Fe-hot spots were reanalyzed for a much longer time.
- The spot to spot variation is significant -- $>10^3$ for Zn, $>10^2$ for Ni.
- A "whole track composition" was determined by averaging these long spectra of the 20 most intense spots in the Fe map, and at hot spots in other element maps (e.g., Ni, Zn).
- **This "whole track composition" (black) differs significantly from that of the terminal particle (blue),** e.g. Ni/Fe ~CI in "whole track" but <0.1xCI in the TP and Cu, Zn, Ga and Se are >CI in the whole track but <<CI in the TP.

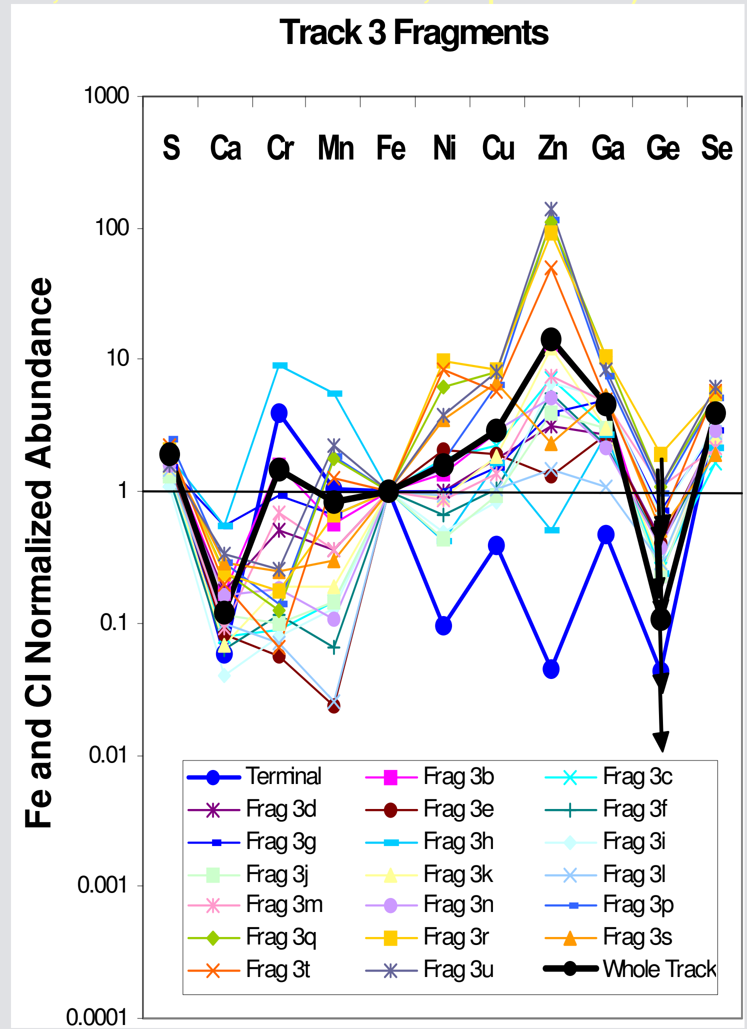

Whole Track Mean Composition

- The Fe-normalized mean composition is within 25% of CI for Ca, Cr, Mn, & Ni, and within 50% for Ti.
- There is a significant S depletion, possibly a statistical effect since ~50% of all the S is in a single track.
- The moderately volatile minor elements Cu, Zn and Ga are enriched (at 1σ and almost at 2σ).
- Ge & Se may be underestimated due to a many non-detections (counted as 0 in the mean).

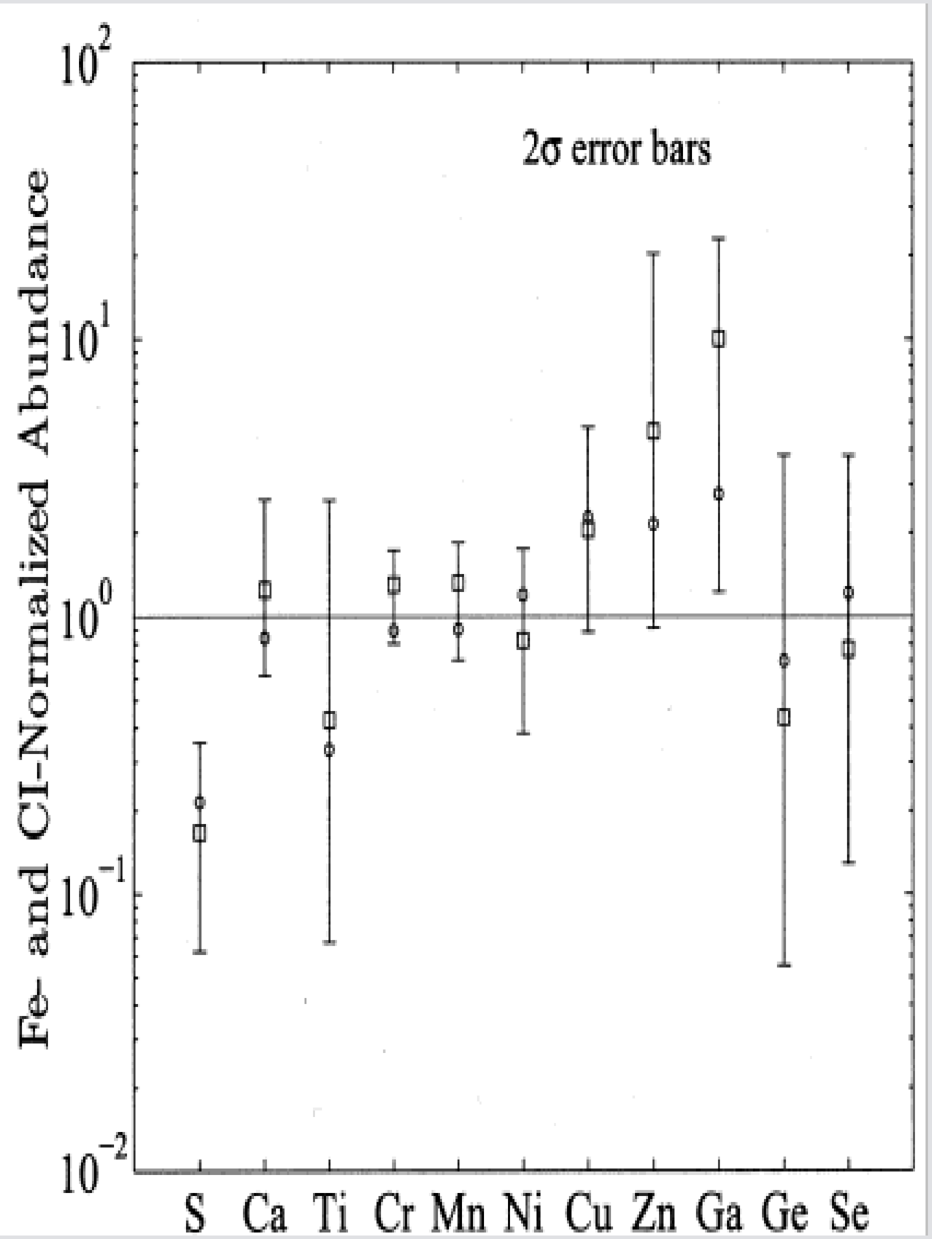

MicroXRD: L2008Z1 Cluster Interplanetary Dust Particle

MAR 345 Image Plate

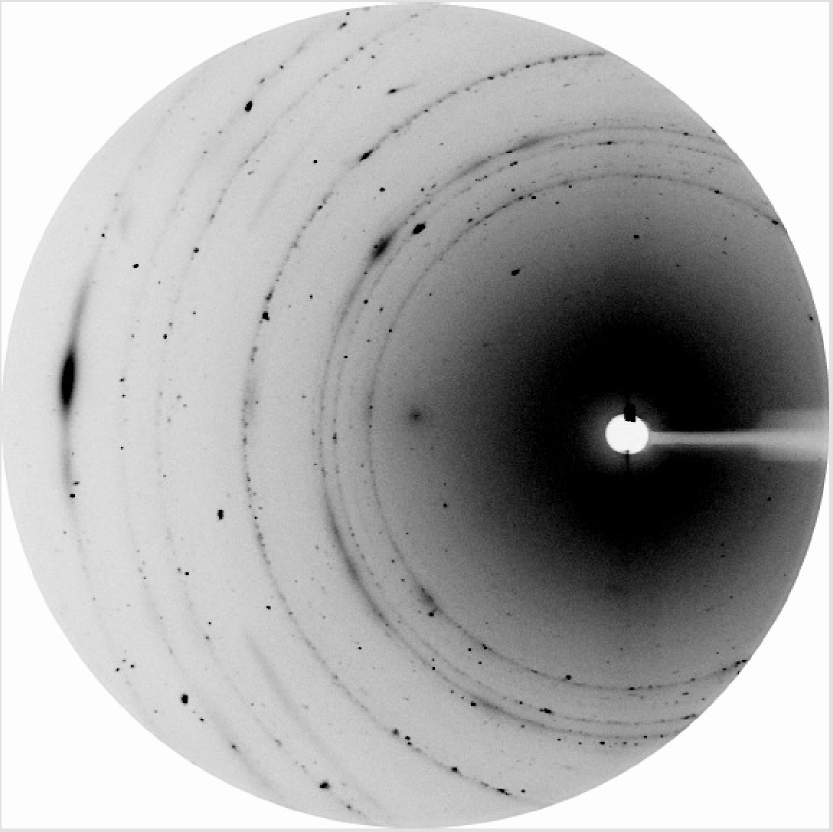

Bruker 1500 CCD

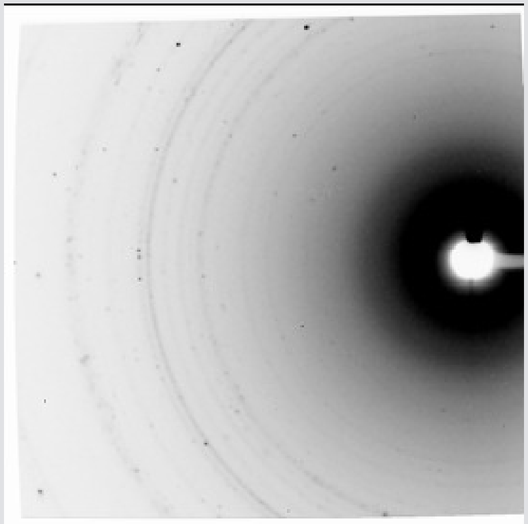

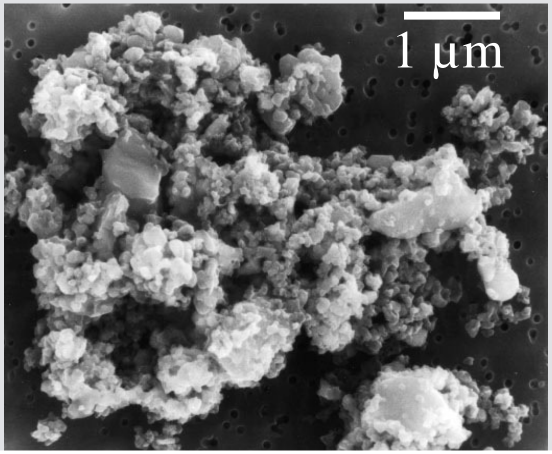

Microprobe Components

Microbeam Optics

- Reflective mirrors (e.g., KB)
- Zone plates
- Bragg-Fresnel lenses
- Compound refractive lenses

Detectors

- Ionization chambers
- Lytle chamber
- Energy dispersive (e.g., Ge, SiLi, Si drift)
- ED arrays (e.g., Canberra Ge)
- Wavelength dispersive (e.g., Oxford WDX)

X-ray Microbeam Production

Advantages of Kirkpatrick-Baez (KB) Microfocusing

- **Achromatic focusing** - focus/beam position is retained during an energy scan
- **Large gain** - gains of > 10^5 achievable, high elemental sensitivity
- **High efficiency** – reflectivity near unity
- **Long working distance** - simplifies use of detectors, optical viewing systems, special sample chambers, etc.
- **Disadvantage** – 0.8 µm beam size achieved but sizes ~ 0.1 µm currently difficult for hard x-rays

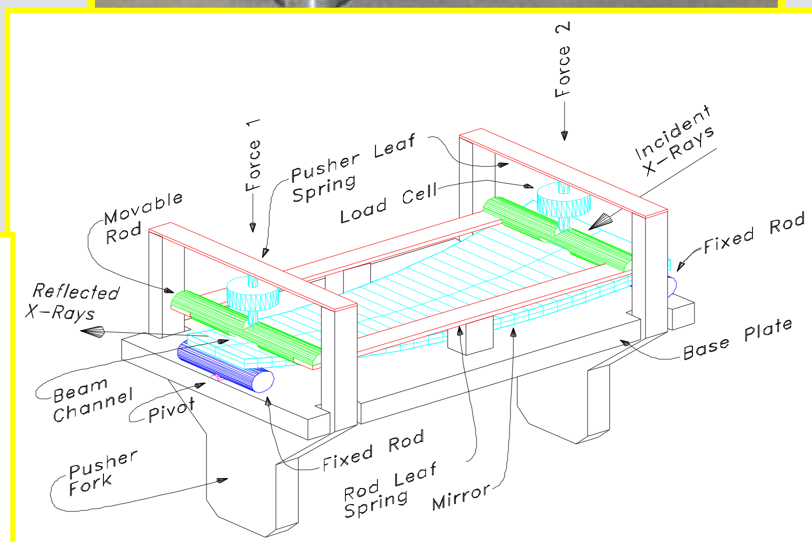

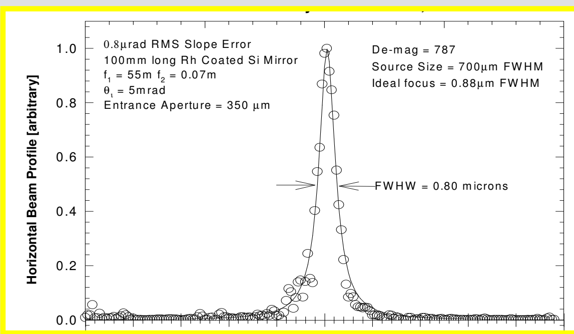

Vortex® multi-cathode x-ray detector (MCD)

- Large single active area (~50 mm^2)
- Cooled by a thermoelectric cooler - can be cycled as frequently - cool down times are typically less than 3 minutes.
- Excellent resolution (<136 eV FWHM at Mn K_α is typical)
- High count rate capability (input rate >1 Mcps).
- At a very short peaking time of 0.1 µs, an output count rate of 600 kcps is achieved.
- High count rates with virtually zero loss in resolution and no peak shift with count rate

SII NanoTechnology USA, Inc

Wavelength Dispersive Spectrometer

(Oxford WDX-600)

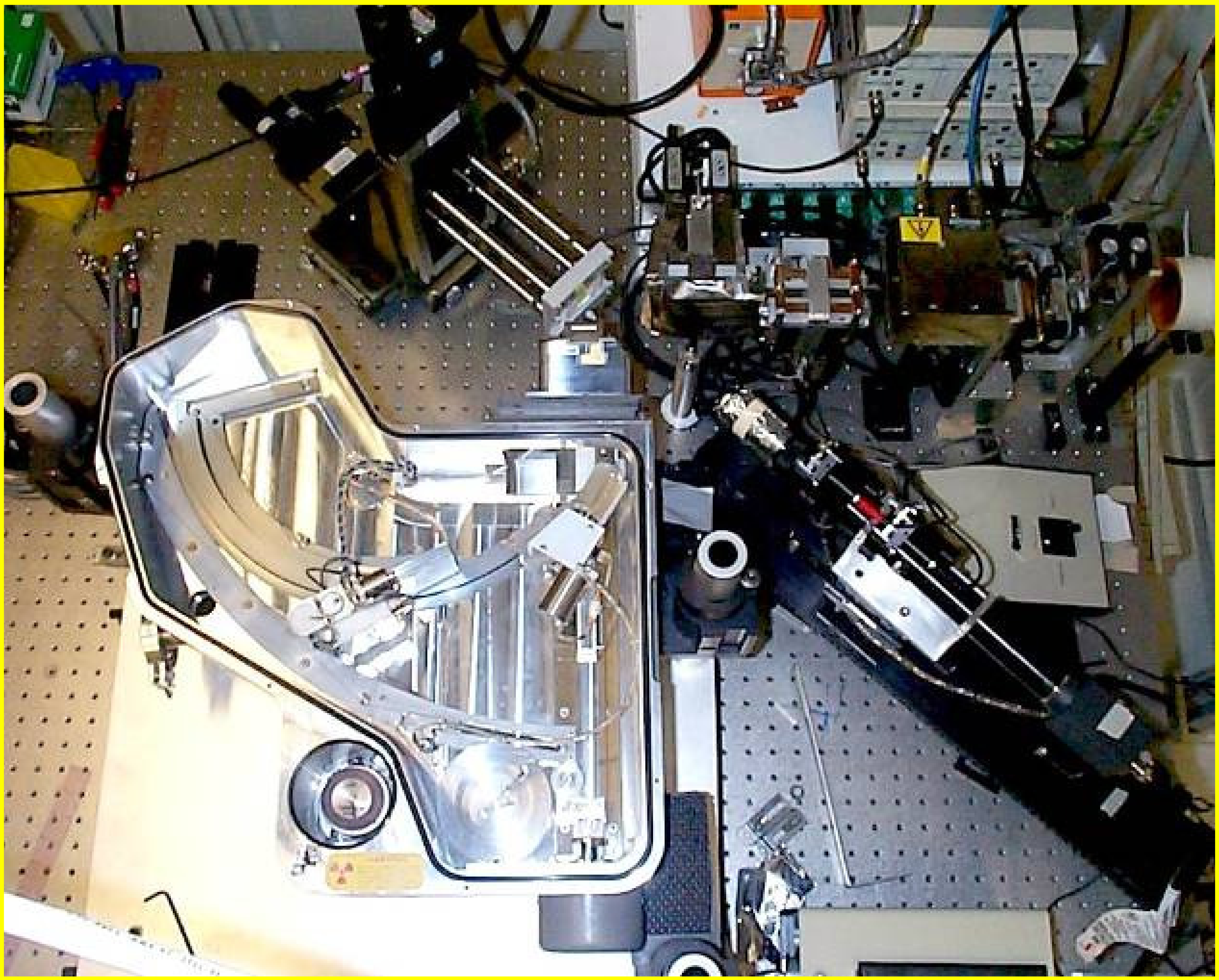

- ~10 times higher energy resolution than SSD
- ~10 times poorer sensitivity than SSD

X-ray Microprobes in Use for Earth and Environmental Science Research

Bending Magnet Source

- KB mirrors; 1-10 μm; 4-25 keV; 10^9-10^{10} ph/sec
- NSLS X26A, X27A; ALS 10.3.2; SSRL 2.3; CAMD; CLS 6-B1, 7-B2

Wiggler Source

- KB mirrors; 2-4 μm; 3-40 keV; 10^9-10^{11} ph/sec
- SSRL 6.2; CLS 6-ID

Undulator Source

- KB mirrors, zone plates, Bragg-Fresnel lenses, compound refractive lenses
- 60 – 5000 nm; 0.6 – 40 keV; 10^9 – 10^{12} ph/sec
- APS 2-ID-D/E, 2-ID-B, 10-ID, 13-ID, 20-ID
- ESRF ID-22, ID-18F; AS BL9; SPring-8 BL37XU, BL47XU; Diamond I18

NSLS Microprobes

Beam Line*	**Managing Agent(s)**	**Scientific Program**	**Source**	**Microbeam Apparatus**	**Energy Range** (keV)	**Beam Size** (µm)	**Flux** (ph/sec)	**Fraction of Beamline used for Earth, Environmental**
NSLS X26A	Univ. of Chicago; Univ. of Georgia; Brookhaven Nat. Lab.	Earth, Environmental	Bending Magnet (2.8 GeV)	KB mirrors	4-30	7	3×10^9	90%
NSLS X27A	Brookhaven Nat. Lab.; Stony Brook University	Earth, Environmental, Physics, Chemistry, Biology	Bending Magnet (2.8 GeV)	KB mirrors	4-20	12	3×10^9	70%

What does “world leading” mean for microprobes?

• Spatial resolution – smaller beams yield greater detail but tunable spatial resolution is generally desirable
• Flux density – hotter beams provide better sensitivity but fragile samples are limited in the power they can take.
• Energy range – broad coverage allows many interacting elements to be studied in the same sample.
• Detectors – move to hotter beams requires move to faster and higher throughput detectors
• Stability – mover to smaller beams requires greater investment in stability control (beam and sample).
• Applicability – samples can be studied “as-is” with no or little preparation.
• Ease of Use – a “world leading” microprobe is easy to use (sample exchange, alignment, tunability, speed, pseudo-real time results).

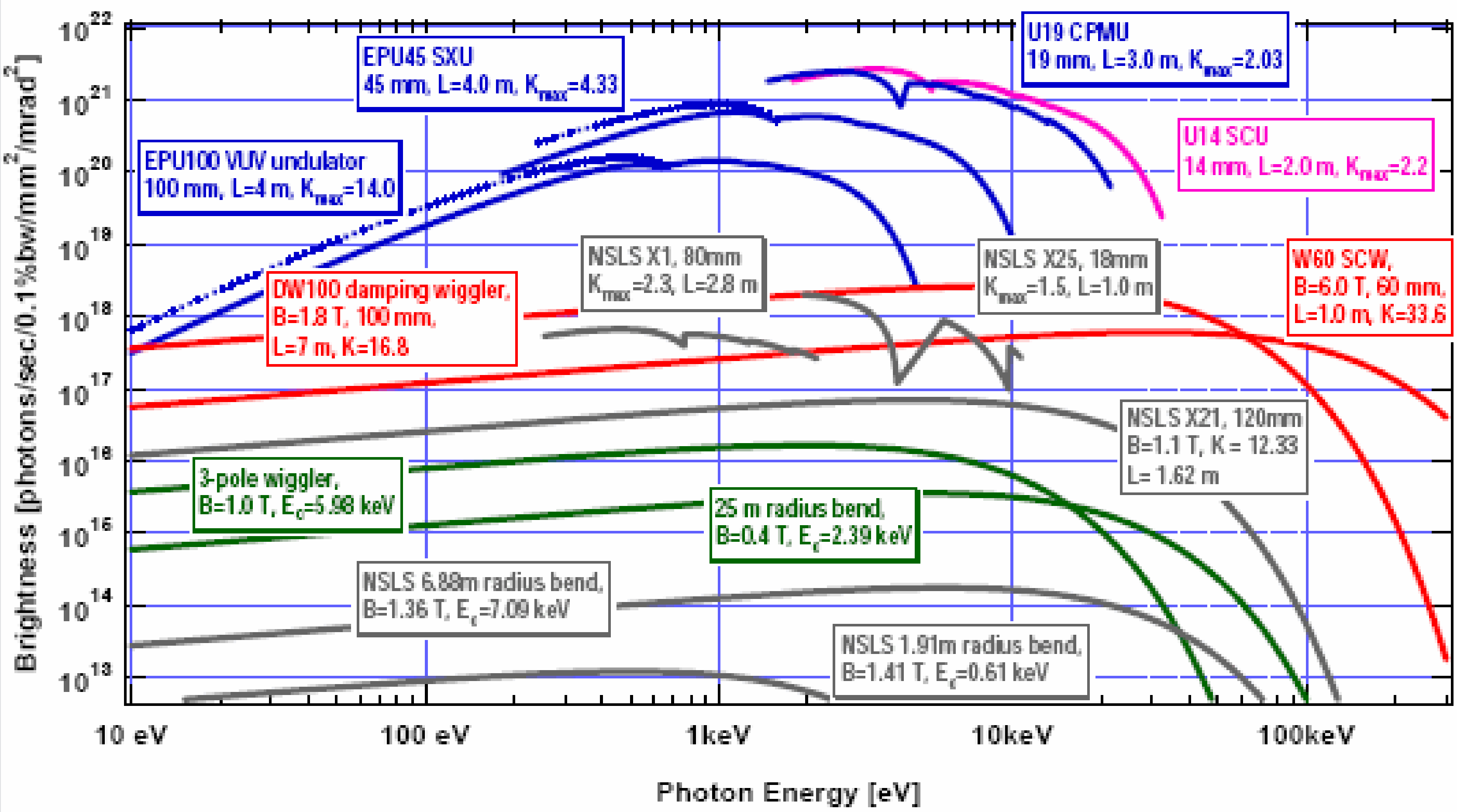

Figure 3. Brightness comparison for NSLS-II and NSLS sources.

U20 and APS UndA Brightness Tuning Curves

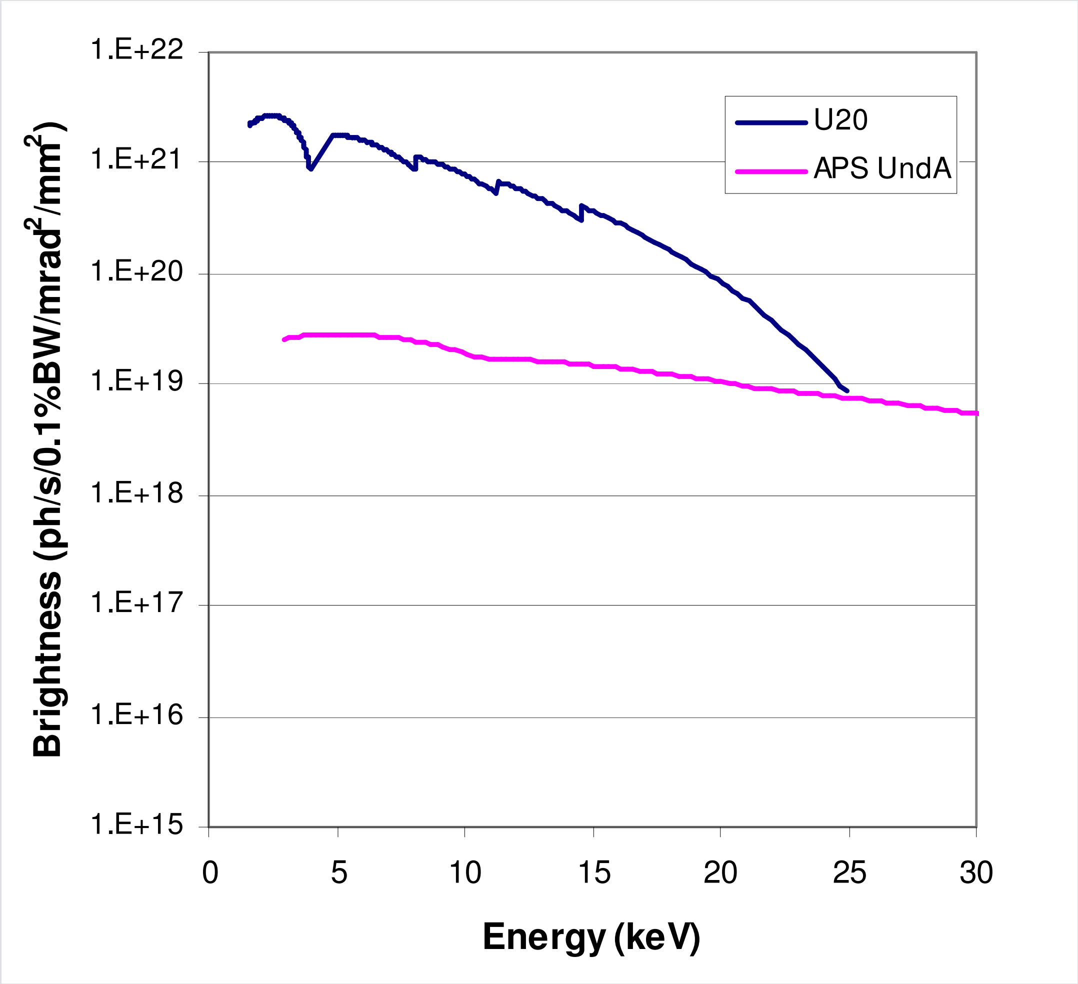

Existing Microprobes: Peak Flux vs Energy Range

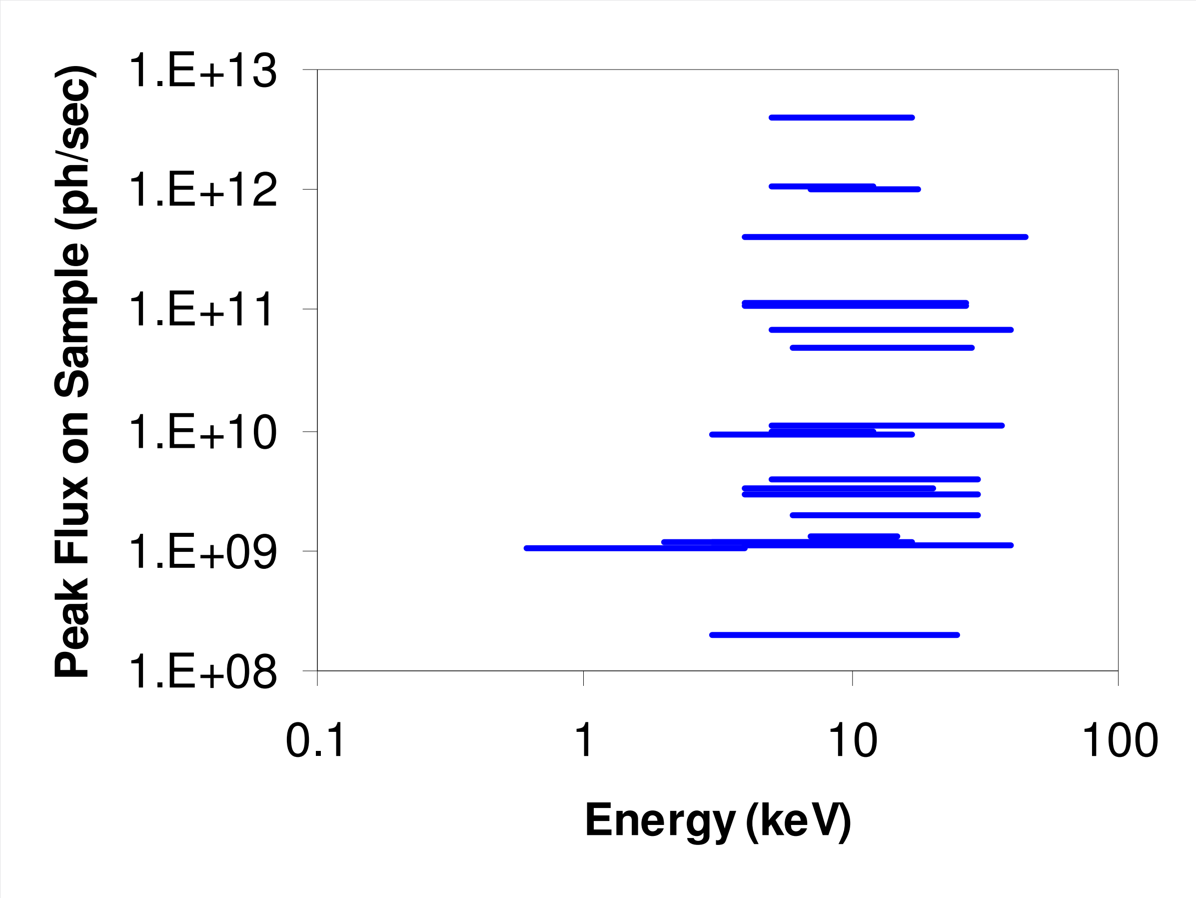

Existing Microprobes: Flux vs Beam Size Characteristics

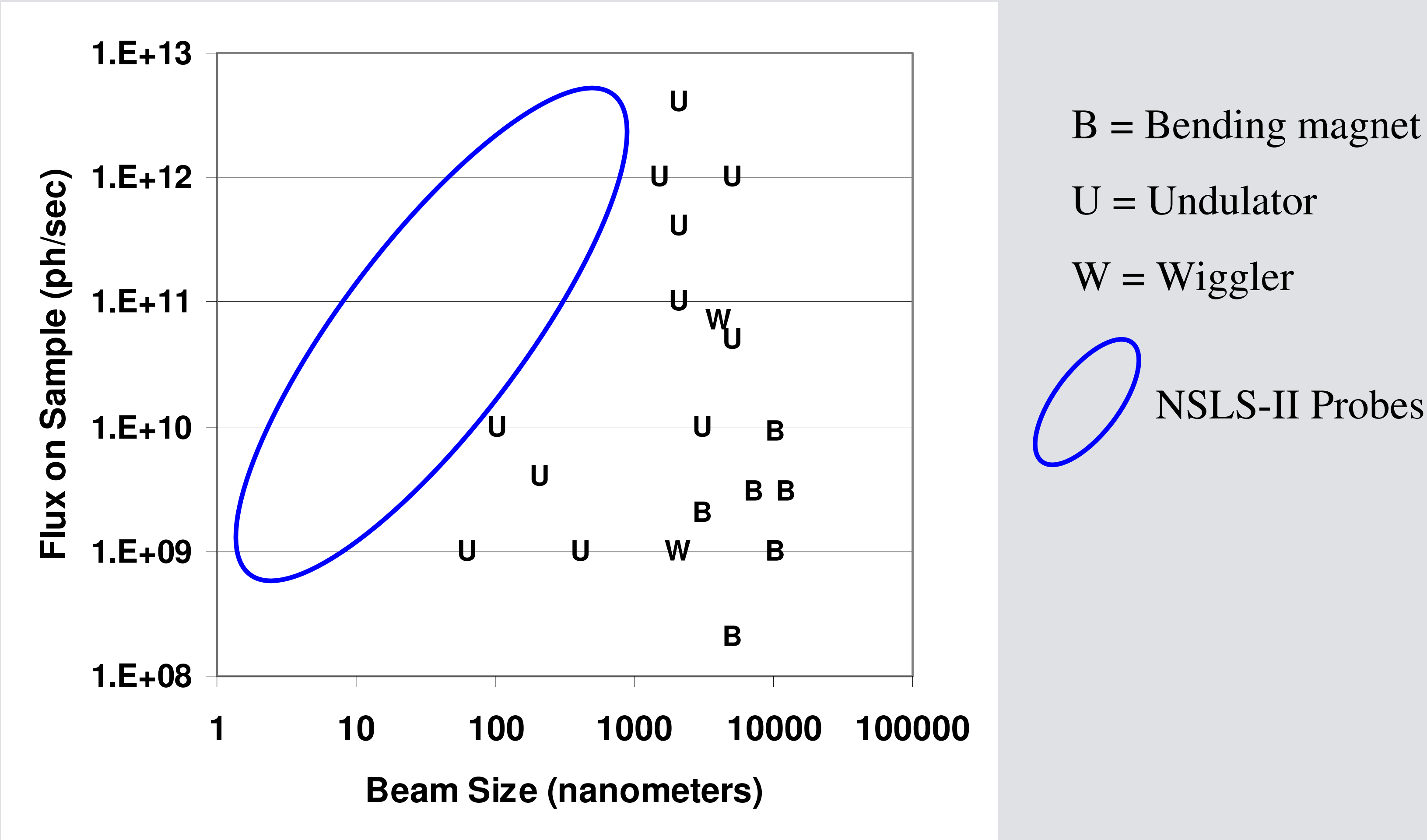

Focusing with Elliptical Mirrors

The demagnification of the source is

$$m = \frac{f_1}{f_2}$$

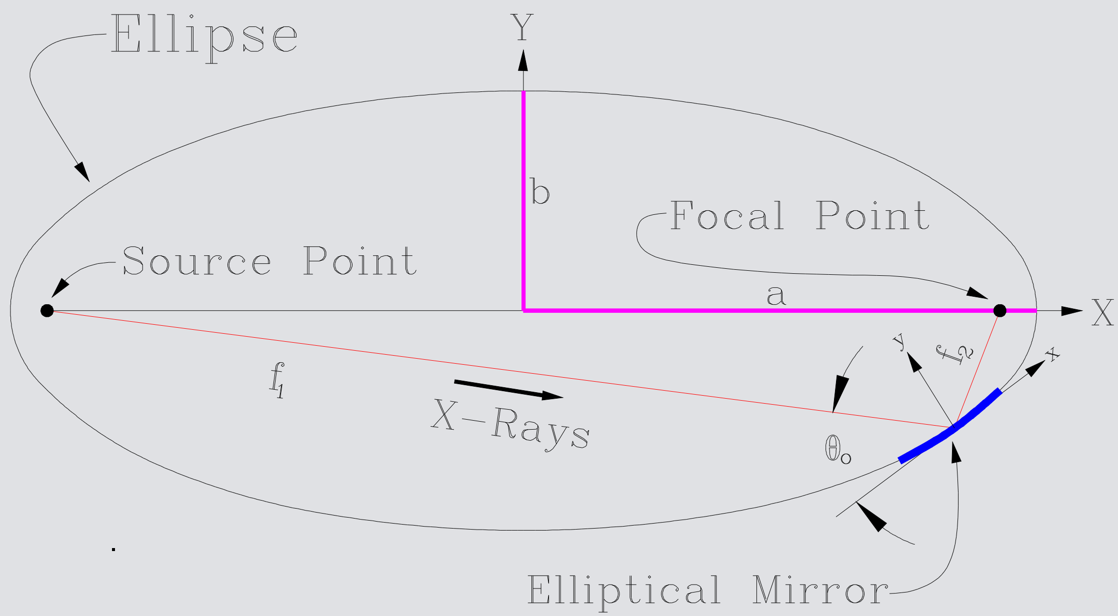

Factor by which the focal image deviates from the ideal is given by:

$$D = \sqrt{\left(\frac{2\sigma'_T}{S'}\right)^2 + 1}\,.$$

Full width at half maximum of the focused beam is:

$$FWHM = 2.35 D \sigma_s / m$$

σ'_T	= mirror's total slope error
σ_s	= source size
$S' = \dfrac{\sigma_s}{f_1}$	angular size of the source

[Eng P. J., et al. (1998) Dynamically figured Kirkpatrick-Baez micro-focusing optics. In X-Ray Microfocusing: Applications and Technique, I. McNulty, ed., SPIE Proc. 3449, 145.]

KB Mirror Focused Beam Sizes for Various Sources (10 keV)

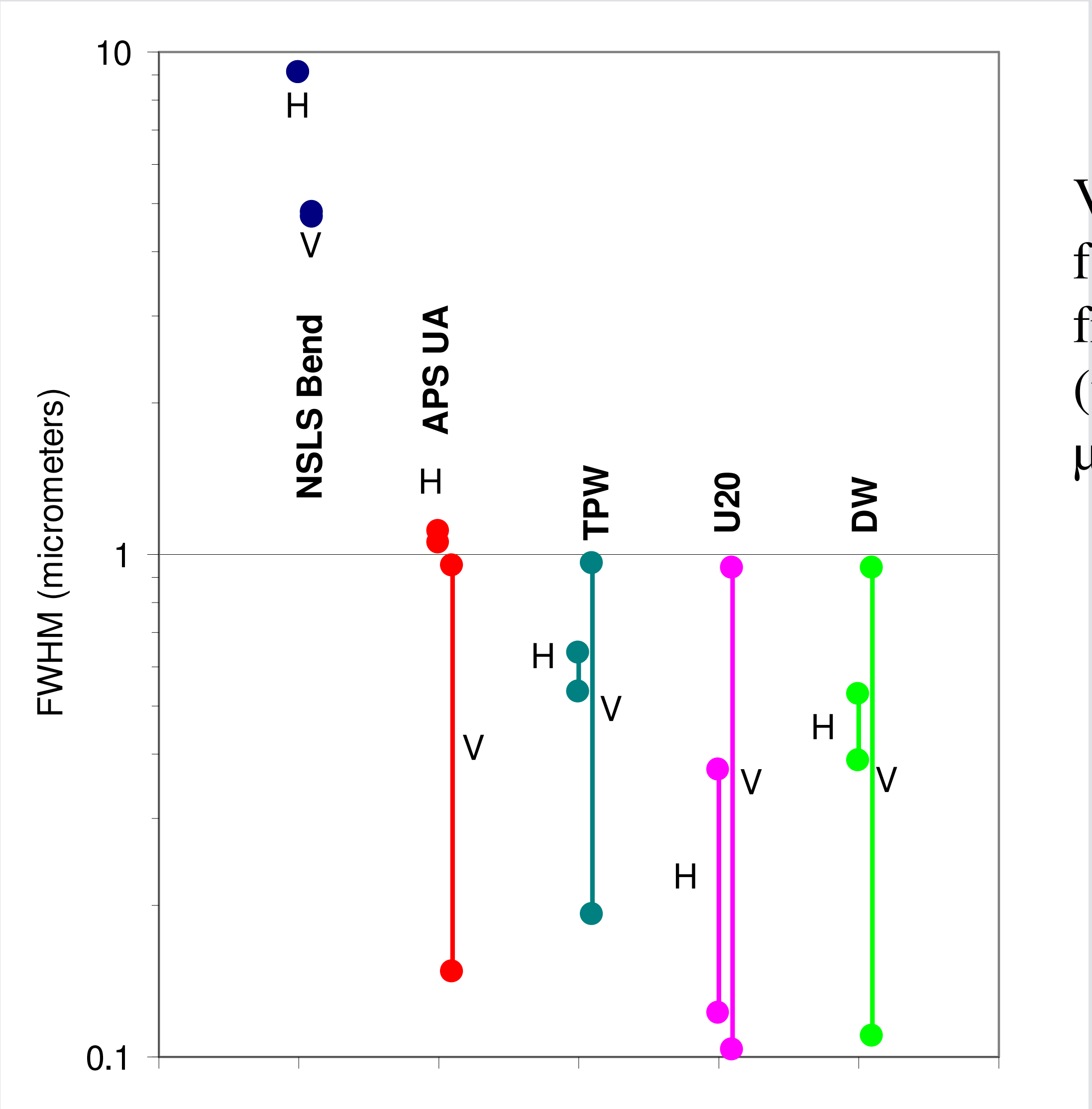

Vertical bars show values for angular deviations from perfect ellipse of 1 (top) and 0.1 (bottom) µrad.

New Microprobe Opportunities at NSLS-II

Mineral interfacial reactions at the sub-grain scale.

• Reactivity, bioavailability, and toxicity of environmental particulates and species adsorbed to particulate surfaces.

• Airborne particulates (cloud condensation nuclei; hydophobic or hydroscopic; aggregation and transport).

• Colloids in natural systems (properties at nanoscale; surface area controls; element cycling in the oceans).

Biogeochemical processes at the nanometer scale.

• Micro- and nano-scale heterogeneity of metals and metalloids in biogeochemical systems.

• Interactions of organisms with contaminants; toxicity and biogeochemistry of manufactured and natural nanoparticles; electron transfer mechanisms between microbes and minerals; cell wall contaminant chemistry; binding mechanisms of natural organic matter and bacteria.

•"Environmental genomics": examine how genetic variations in organisms affect their interactions with contaminant and nutrient metal species in the environment; help evaluate how specific genes influence the uptake of metals in plants and animals.

New Microprobe Opportunities at NSLS-II (continued)

Fluid flow and contaminant transport at the pore scale.

- Imaging mineral-solution reactions in confined spaces *in-situ* within dense geologic media.
- Direct observations of pore scale transport may be possible, particularly in 3-dimensions using spatially resolved tomographic techniques.
- Image and quantify the distribution of pore spaces, evaluate microbial distribution on pore walls, and micro-spectroscopically evaluate colloidal chemistry at mineral interfaces.

In-situ x-ray diffraction of environmental materials.

- Real-time scattering to follow phase evolution as a function of time and environmental conditions (P, T, Eh, pH, fO_2 etc.).
- Mimic the conditions under which naturally occurring and engineered materials operate, compare engineered samples and environments with those found in nature.

General Microprobe Requirements

- Wide energy range required
- Variable beam size (e.g., via variable secondary focus)
- High degree of stability (apparatus and samples)
- Environmental chambers (apparatus flexibility is crucial)
- High throughput detectors with high energy resolution
- Fast data collection especially for mapping
- User friendly software for data collection and analysis